Equivalent photons in proton-proton and ion-ion collisions at the LHC

E. V. Zhemchugov
Institute for Theoretical and Experimental Physics, 117218, Moscow, Russia
Moscow Engineering Physics Institute, 115409, Moscow, Russia

Equivalent photon approximation is used to provide theoretical description of muon pair production in ultraperipheral proton-proton and ion-ion collisions taking into account electromagnetic form factors of colliding particles. Analytical formula for the fiducial cross section is presented. Calculations are compared to experimental results provided by the ATLAS collaboration. Prospects of finding New Physics in proton-proton and ion-ion collisions are compared. A strategy for the search of new heavy long-lived charged particles in ultraperipheral collisions with the help of the forward detectors is proposed.

1 Introduction

Ultraperipheral collisions (UPC) constitute a large fraction of collisions at the Large Hadron Collider (LHC). In this kind of collisions the colliding particles pass near each other at some distance and collide with their electromagnetic fields. The particles remain intact after the collision and may be registered in a special pair of forward detectors placed further down the beam (ATLAS Forward Proton Detector or CMS-TOTEM Precision Proton Spectrometer). The LHC may be considered as a photon-photon collider with the photon collisions happening in the UPCs.

Leading order Feynman diagrams describing muon pair production in an UPC are shown in Fig. 1. Cross section of any UPC is proportional to Z^4 where Z is the charge of the colliding

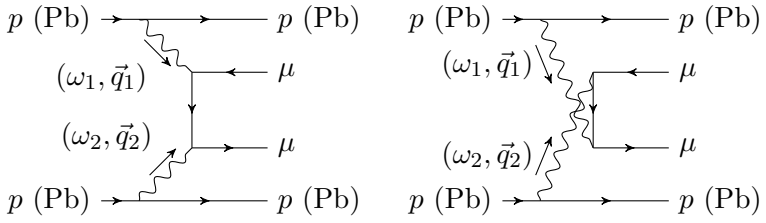

Figure 1: Leading order Feynman diagrams for the $pp(\gamma\gamma) \to pp\mu^+\mu^-$ (Pb Pb $\to$ Pb Pb $\mu^+\mu^-$) reaction.

particle. For Pb, this value is of the same order (10^7) as the ratio of the integrated luminosity collected so far in *pp* collisions to Pb Pb collisions: 159 fb^{-1} of *pp* collisions in 21 months of Run 2 and 2.4 nb^{-1} of Pb Pb collisions in 2 months of heavy ion runs in 2015 and 2018 [1,2]. The LHC luminosity in Pb Pb collisions can be easily increased and thus they look quite promising for the search of New Physics that can appear in photon-photon collisions. Let us further compare the properties of *pp* and Pb Pb UPCs.

2 Equivalent photon approximation

To describe an UPC, the equivalent photon approximation (EPA) is commonly used [3,4,5,6] (see also [7,8,9,10]). In the EPA, the electromagnetic field of an ultrarelativistic charged particle is replaced with a bunch of approximately real photons distributed according to the spectrum

$$n(\omega) = \frac{2Z^2\alpha}{\pi\omega} \int\limits_0^\infty \frac{q_\perp^3 F^2(q_\perp^2 + \omega^2/\gamma^2)}{(q_\perp^2 + \omega^2/\gamma^2)^2} \mathrm{d}q_\perp, \tag{1}$$

where ω is the photon energy, $q_\perp$ is the photon transverse momentum, γ is the Lorentz factor of the source particle and F is its electromagnetic form factor. In the case of proton, F can be approximated with the dipole formula, and the integral can be performed analytically [11]:

$$F(\vec{q}^{\,2}) = \frac{1}{(1 + \vec{q}^{\,2}/\Lambda_2^2)^2}, \qquad n_p(\omega) = \frac{\alpha}{\pi\omega} \left[(4a+1) \ln\left(1 + \frac{1}{a}\right) - \frac{24a^2 + 42a + 17}{6(a+1)^2} \right], \tag{2}$$

where $a = (\omega/\Lambda_2\gamma)$, $\vec{q}$ is the photon 3-momentum in the proton rest frame, $\Lambda_2 = 0.84$ GeV [12].

Heavy nucleus form factor is described through coefficients of its Fourier-Bessel decomposition [13]. There are two sets of coefficients for ^{208}Pb available in the literature [14,15].[a] In UPCs, only the low-energy behaviour of the form factor is important. Approximation of the form factor with monopole formula results in the following spectrum [11]:

$$F(\vec{q}^{\,2}) = \frac{1}{1 + \vec{q}^{\,2}/\Lambda_1^2}, \qquad n_{\text{monopole}}(\omega) = \frac{Z^2\alpha}{\pi\omega} \left[(2a+1) \ln\left(1 + \frac{1}{a}\right) - 2 \right], \tag{3}$$

where Λ_1 is either 80 MeV [11,14] or 50 MeV [11,15]. EPA spectra of a 6.5 TeV proton and 522 TeV ^{208}Pb (the current LHC energies) are presented in Fig. 2b. At high photon energies the form factor cuts off the spectrum. Heavy nucleus advantage of high electric charge diminishes for photons with the energies higher than 200–400 GeV.

The UPC cross section is the photon-photon collision cross section convoluted with the photon spectra:

$$\sigma(NN \to NN\,\mu^+\mu^-) = \int_0^\infty \int_0^\infty \sigma(\gamma\gamma \to \mu^+\mu^-)\, n_N(\omega_1)\, n_N(\omega_2)\, \mathrm{d}\omega_1 \mathrm{d}\omega_2, \tag{4}$$

where N is the colliding particle. In an experiment, some regions of the phase space of the particles produced in a collision are unavailable. Common requirements for the event to be registered are: particle pseudorapidity η is such that the particle hits some detector system (e.g., the muon system): $|\eta| < \hat{\eta}$; particle transverse momentum p_T is such that the signal is not dominated by the background: $p_T > \hat{p}_T$; the system invariant mass $\sqrt{s} = \sqrt{4\omega_1\omega_2}$ is in

[a] Fourier-Bessel coefficients for ^{208}Pb provided in the latter paper [15] appear to be not self-consistent: $\langle r^2 \rangle^{1/2} = \int \rho(r) r^2\, \mathrm{d}^3 r / \int \rho(r)\, \mathrm{d}^3 r = 7.74$ fm when calculated through the coefficients which does not equal to 5.4785 fm presented in same the table (here $\rho(r)$ is the nucleus charge density). In the former paper [14] these values are equal.

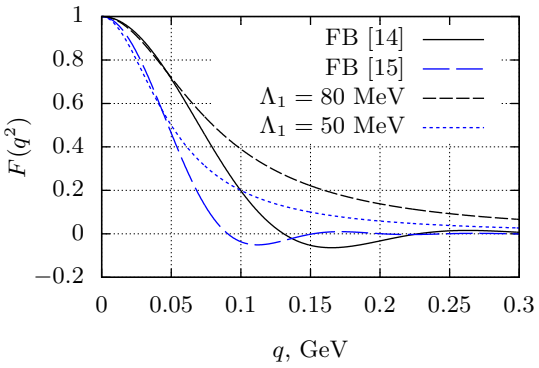

(a) ^{208}Pb form factor. "FB [14]" and "FB [15]" are Fourier-Bessel decompositions [14,15]. "Λ_1" are monopole approximations (3) with the corresponding value of Λ_1.

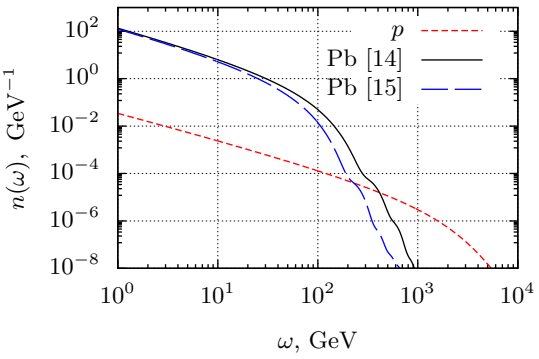

(b) EPA spectra of a 6.5 TeV proton (2) and 522 TeV ^{208}Pb with the form factors calculated through Fourier-Bessel decompositions [14,15].

some available range: $\hat{s}_{\min} < s < \hat{s}_{\max}$. These experimental cuts can be taken into account analytically [11]:

$$\sigma_{\text{fid.}}(NN \to NN\,\mu^+\mu^-) = \int\limits_{\hat{s}_{\min}}^{\hat{s}_{\max}} \mathrm{d}s \int\limits_{\hat{p}_T}^{\sqrt{s}/2} \mathrm{d}p_T \frac{\mathrm{d}\sigma(\gamma\gamma \to \mu^+\mu^-)}{\mathrm{d}p_T} \int\limits_{1/\hat{x}}^{\hat{x}} \frac{\mathrm{d}x}{8x}\, n_N\left(\sqrt{\frac{sx}{4}}\right) n_N\left(\sqrt{\frac{s}{4x}}\right), \tag{5}$$

where $\sigma_{\text{fid.}}$ is the fiducial cross section, $x = \omega_1/\omega_2$, $\hat{x} = \mathrm{e}^{2\hat{\eta}} \frac{1-\sqrt{1-4\hat{p}_T^2/s}}{1+\sqrt{1-4\hat{p}_T^2/s}}$.

3 Comparison to experiment

The ATLAS collaboration has measured fiducial cross sections for muon pair production in pp and Pb Pb ultraperipheral collisions [16,17].

For the pp collisions, the cut on muon pseudorapidity was $|\eta| < \hat{\eta} = 2.4$, and the cut on muon transverse momentum was $p_T > \hat{p}_T = 6$ GeV for 12 GeV $< \sqrt{s} <$ 30 GeV and $\hat{p}_T = 10$ GeV for 30 GeV $< \sqrt{s} <$ 70 GeV. Comparison of calculations with the help of Eq. (5) to the experimental data is presented in Fig. 3a [11].

In the case of Pb Pb collisions, the cuts were as follows: $\hat{\eta} = 2.4$, $\hat{p}_T = 4$ GeV for 10 GeV $< \sqrt{s} <$ 100 GeV. Comparison with the experimental data is presented in Fig. 3b [11].

The calculations presented here do not take into account the sizes of the colliding particles. With the sizes taken into account the pp cross sections should be reduced by 10–20% [18], and the Pb Pb cross sections should be reduced by a larger factor [19]. In spite of the calculation with the form factor from the latter paper [15] so nicely matching the experimental points in Fig. 3b, form factor from the earlier paper [14] appears to have more accurate low-energy behaviour.

4 New Physics

In UPCs, production of new particles is mediated by photons. Z boson exchange is suppressed by the long distance between the colliding particles. Consequently, production cross section depends only on the charges and the masses of the produced particles and is not sensitive to other model parameters. Thus, UPCs provide unique opportunity for the search of new particles carrying an electric charge compared to inclusive production processes that are always contaminated by the interference with the Z boson and possibly other New Physics bosons (higgsinos, Z', etc.). In particular, UPCs are well suited for the search of heavy long-lived charged particles that occur in some models of New Physics. For example, in supersymmetry, the lightest chargino might

be long-living if the mass difference between the lightest neutralino and the lightest chargino is less than 2 GeV.

There are many searches of long-lived charged particles (LLCP) . Most of them consider the minimal supersymmetric model (MSSM), and all of them set model-dependent bounds on the LLCP mass. UPC bounds will be model-independent.

Production of a pair of LLCPs in an UPC is a very clean process, since in the final state there are only 4 particles: the initial protons or heavy ions, and two LLCPs leaving a track in the detector. The protons can be registered in forward detectors (lead ions will not survive the high energy loss required [20]). The LLCPs momenta can be measured from their tracks curvatures, just like it is done for the muons. In this case full kinematics of the process can be reconstructed and the LLCP mass can be calculated. This approach is different from and may be considered as complementary to the conventional searches for LLCPs based on their ionization energy losses and time-of-flight measurements.

Let E be the energy of each proton before the collision, $\xi_1 E$ and $\xi_2 E$ are the protons energies after the collision measured by the forward detectors, $\vec{p}_1$ and $\vec{p}_2$ are LLCPs momenta measured from their tracks in the central detector. Then the LLCP mass is [20]

$$m = \sqrt{\frac{(2\xi_1\xi_2 E^2 + \vec{p}_1\vec{p}_2)^2 - \vec{p}_1^{\,2}\vec{p}_2^{\,2}}{4\xi_1\xi_2 E^2 + (\vec{p}_1 + \vec{p}_2)^2}}. \tag{6}$$

Calculating this value for every event with exactly two charged tracks and two protons detected in forward detectors, and plotting the number of such events with respect to m, one should get $\delta(m - m_\chi)$ (where m_χ is the mass of the LLCP) smeared with the detector resolution.

The important source of background in this approach is production of a pair of muons which also leave two tracks in detector and can thus mimic production of a LLCP pair. This background is enhanced when multiple collisions occur at the same time (pile-up), since forward detectors cannot tell which vertex the proton came from. The total 3-momenta of the system is known, and the background is severely suppressed by a cut on the longitudinal component of the system momentum [20]:

$$|p_{\parallel,1} + p_{\parallel,2} - (\xi_1 - \xi_2)E| < 20 \text{ GeV}. \tag{7}$$

LLCP pair production cross section in an UPC of protons or lead ions with the current LHC parameters is shown in Fig. 4a [20]. LLCP ($\tilde{\chi}_1^{\pm}$) mass distribution for $m_\chi = 100$ GeV and for the

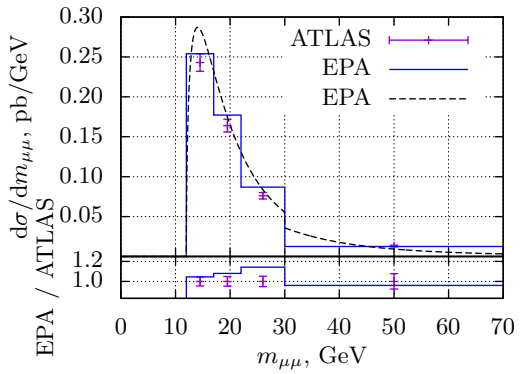

(a) *Upper plot:* fiducial cross section for the $pp \to pp\,\mu^+\mu^-$ reaction. The points are experimental data [16]. The dashed line is the differential cross section (5). The histogram is the cross section integrated over experimental bins. *Lower plot:* ratio of the calculated cross section to the experimental points.

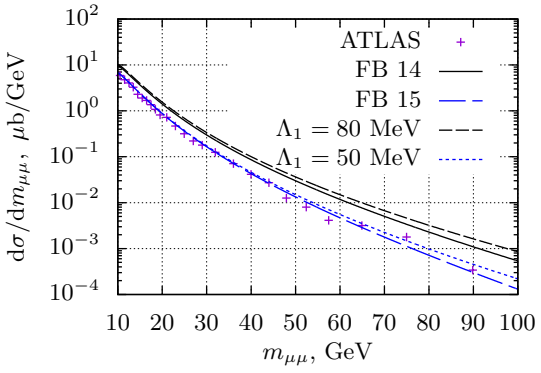

(b) Fiducial cross section for the $\mathrm{Pb\,Pb} \to \mathrm{Pb\,Pb}\,\mu^+\mu^-$ reaction. The points are experimental data [17]. The solid lines are the cross section (5) calculated with the form factors represented as Fourier-Bessel decompositions [14,15]. The dashed lines are monopole approximations (3).

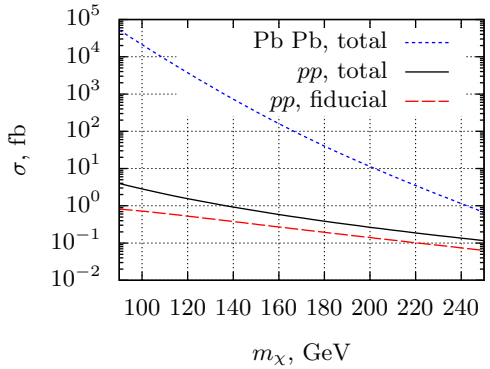

(a) LLCP pair production cross section. "total" is the cross section for the whole phase space, while "fiducial" is the cross section with the requirement that both protons hit the forward detectors and both LLCPs have $p_T > 20$ GeV, $|\eta| < 2.5$.

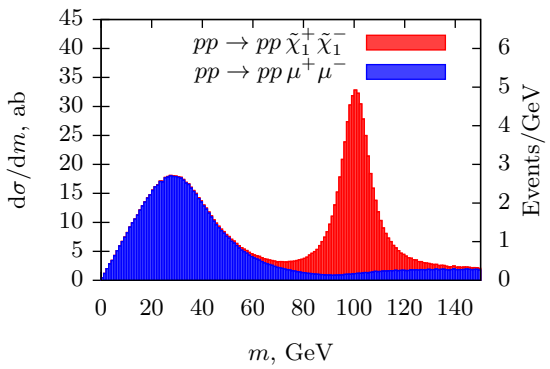

(b) LLCP candidate mass distribution (6) with constant pile-up of 50 collisions at once and extra cut (7). The integrated luminosity is 150 fb^{-1}.

ATLAS detector resolution, assuming constant pile-up of 50 collisions at once is presented in Fig. 4b [20].

5 Conclusions

Cross section of ultraperipheral collisions is enhanced by high electric charge of the colliding particles but is suppressed by their electromagnetic form factor. Available photon energies are ~ 1 TeV for a 6.5 TeV proton and ~ 100 GeV for a 522 TeV ^{208}Pb. With the current LHC energies, when production of a system with invariant mass greater than 400–800 GeV is required, lead ions have no advantage over protons.

Fiducial cross section for production of a pair of charged particles in an UPC with typical cuts on the phase space is described with analytical formulas. Calculations are within experimental errors for the $pp \to pp\,\mu^+\mu^-$ reaction. For the Pb Pb $\to$ Pb Pb $\mu^+\mu^-$ reaction, the sizes of colliding particles have to be taken into account.

Ultraperipheral collisions can set model-independent limits on the masses of possible new charged particles. When a pair of long-lived charged particles is produced in an ultraperipheral collision of protons, full kinematics of the process can be reconstructed with no need for ionization energy loss or time-of-flight measurements.

I am grateful to the organizers for an inspiring conference and an opportunity to visit again this beautiful town. I am supported by the Russian Foundation Grant No 19-12-00123.

1. ATLAS Luminosity—Public Results. https://twiki.cern.ch/twiki/bin/view/AtlasPublic/LuminosityPublicResultsRun2
2. CMS Luminosity—Public Results. https://twiki.cern.ch/twiki/bin/view/CMSPublic/LumiPublicResults
3. E. Fermi. Z.Physik 29, 315 (1924).
4. C. F. V. Weizsäcker. Z.Physik 88, 612 (1934).
5. E. J. Williams. Kgl. Danske Vidensk. Selskab. Mat.-Fiz. Medd. 13, 4 (1935).
6. L. D. Landau, E. M. Lifshitz. Phys.Zs.Sowjet 6, 244 (1934).
7. V. E. Balakin, V. M. Budnev, I. F. Ginzburg. JETP Lett. 11, 388 (1970).
8. H. Terazawa. Rev.Mod.Phys. 4, 615 (1973).
9. V. M. Budnev, I. F. Ginzburg, G. V. Meledin, V. G. Serbo. Particles & Nuclei 4, 239 (1973) [in Russian].
10. V. M. Budnev, I. F. Ginzburg, G. V. Meledin, V. G. Serbo. Phys.Rep. 15, 181 (1975)

11. M. Vysotsky, E. Zhemchugov. Accepted to Physics-Uspekhi. arXiv:1806.07238
12. S. Pacetti, R. B. Ferroli, E. Tomasi-Gustafsson. Phys.Rep. 550, 1 (2015).
13. B. Dreher, J. Friedrech, K. Merle, H. Rothhaas, G. Lührs. Nucl.Phys. A235, 219 (1974).
14. H. de Vries, C. W. de Jager, C. de Vries. Atomic Data and Nuclear Data Tables 36, 495 (1987).
15. G. Fricke, C. Bernhardt, K. Heilig, L. A. Schaller *et al.* Atomic Data and Nuclear Data Tables 60, 177 (1995).
16. The ATLAS Collaboration. Phys.Lett. B 777, 303 (2018). arXiv:1708.04053
17. The ATLAS Collaboration. ATLAS-CONF-2016-025 (2016).
18. M. Dyndal, L. Schoeffel. Phys.Lett.B 741, 66 (2015). arXiv:1410.2983
19. R. N. Cahn, J. D. Jackson. Phys. Rev. D42, 3690 (1990).
20. S. I. Godunov, V. A. Novikov, M. I. Vysotsky, E. V. Zhemchugov. arXiv:1906.08568